Robotica (1998) volume 16, pp. 11–21. Printed in the United Kingdom © 1998 Cambridge University Press

Model-based control of rigid-link flexible-joint robots: an experimental evaluation*†

M.S. de Queiroz, S. Donepudi, T. Burg, and D.M. Dawson

Department of Electrical and Computer Engineering, Center for Advanced Manufacturing, Clemson University, Clemson, SC 29634-0915 (USA)

(Received in Final Form: May 23, 1997)

SUMMARY

In this paper, we present an experimental evaluation of several link position tracking control algorithms for rigid-link flexible-joint robot manipulators. To study the performance of the controllers, an IMI 2-link direct-drive planar robot manipulator was modified to approximate linear torsional spring couplings from the actuators to the links. Preliminary experimental results seem to indicate that reduced-order, model-based controllers with an actuator feedback loop provide relatively good link position tracking while a full-order, model-based controller offers some further improvement in link position tracking at the expense of increased computation.

1 INTRODUCTION

In order to obtain a better link position tracking performance in robot manipulators, many control researchers have suggested that the effects of the robot joint flexibility should be included during the modeling process and the subsequent control synthesis. Indeed, early experimental work[2–4] suggest that joint flexibility effects can limit the robustness and performance of a given robot controller. By modeling the joint flexibility as a simple linear spring, Spong[5] proposed a globally feedback linearizable rigid-link flexible-joint (RLFJ) robot model that reduces to the standard rigid-link (RL) robot model as the joint stiffness tends to infinity. As a result, this RLFJ model has been widely utilized by the robotic control research community for the design of robot controllers. For example, Ghorbel et al.[6] used singular perturbation techniques to motivate how a high-gain actuator feedback term can be used to augment standard RL controllers (see [7] also). Experimental results on a 1 degree-of-freedom (DOF) RLFJ robot indicated that this actuator feedback term improves link position setpoint/tracking performance (also see reference 8). Since the work given in references 6–8, involves the use of a high-gain actuator feedback control term to justify using a reduced-order model for control design purposes, many researchers have postulated that improved link position tracking performance might be attained if the full-order model is used for the control synthesis. For example, references 9 & 10, and several of the references therein, researchers have used backstepping, passivity, and feedback linearization techniques to design controllers for the full-order RLFJ model proposed in reference [5].

Based on our assessment of the literature, there seems to be little work regarding the experimental evaluation of controllers for multi-DOF RLFJ robot manipulators.‡ Furthermore, we are not aware of any experimental work which illustrates the expected increase in link position tracking performance of a full-order, model-based control scheme over reduced-order, model-based control schemes. One possible reason for the lack of experimental data for RLFJ controllers could be attributed to the difficulty of procuring a suitable experimental testbed which resembles the RLFJ model given in reference [5]. In much of the RLFJ control literature, harmonic drives are often cited as one of the major causes of joint flexibility. However, in the experimental studies[12–15] it was shown that the dynamic behavior of harmonic drive gearing is much more complex than that of a linear spring. Specifically,[14] it has been shown that a harmonic drive can be modeled as a nonlinear spring which reduces to the standard linear spring model under certain assumptions. Bridges et al.[16] presented an experimental investigation which indicated that the resonant effects introduced by harmonic drive gearing is a more severe problem than joint flexibility-induced link position tracking error and other high gain-induced instability effects; hence, a more detailed model must be used for the development of control strategies for robot manipulators with harmonic drives (see reference [17] for such a presentation). As the facts described above seem to indicate, additional effects introduced by harmonic drives in robot systems

* A preliminary version of this paper appeared in reference 1.

† This work is supported in part by the U.S. National Science Foundation Grants DMI-9457967, DDM-931133269, DOE Contract No. DE-AC21-92MC29115, the Office of Naval Research Grant URI-3139-YIP01, the Union Camp Corporation, the AT&T Foundation, and the National Research Council-CNPq (Brazil).

‡ Recently, Brogliato et al.[11] presented an experimental comparison of several globally stable RLFJ controllers utilizing a 2-DOF robot testbed which contains only *one* flexible joint.

contaminate the proper experimental evaluation of RLFJ controllers based on the model given in reference [5].

The objective of this paper is to investigate the expected performance gains of a full-order, model-based RLFJ controller while also presenting experimental data for reduced-order, model-based controllers on a 2-DOF, flexible joint, robot manipulator. To accomplish this objective, we first construct an experimental RLFJ robot testbed which allows the effects of joint flexibility to be studied without corruption from the effects of standard gearing (i.e. backlash) or harmonic drives; hence, the testbed closely resembles the model presented in reference [5] (i.e. a torque-input, robot manipulator with linear torsion springs between the actuators and the links and an additional set of encoders on the links). While this RLFJ experimental setup might not represent an actual robot system, it does provide a good testbed for evaluating the performance of model-based RLFJ controllers and to investigate the usefulness of the control structure (e.g. the effects of feedforward terms or the use of model-based velocity observers). It is important to note that any controller designed for the RLFJ model of reference [5] will certainly constitute the inner core of a model-based controller designed for the RLFJ model augmented by the effects of harmonic drive gearing;* hence, the experimental results presented in this paper may predict the experimental results of future reduced-order and full-order controllers designed for RLFJ harmonic drive robots.

The paper is organized as follows: In Section 2, we present the standard RLFJ robot dynamic model. In Section 3, we heuristically motivate the design of controllers based on a reduced-order RLFJ model. Section 4 contains the description of two commonly used techniques for synthesizing velocity measurements from position measurements. In Section 5, we briefly discuss the construction of a full-order model-based RLFJ controller. Section 6 describes the experimental RLFJ testbed and presents the experimental results for three reduced-order model-based controllers and one full-order model-based controller. Some concluding remarks regarding the performance of the controllers are given in Section 7.

* In fact, the control design of reference 17 is, roughly speaking, composed of a robust controller previously developed for the RLFJ model of reference 5 augmented with additional terms due to the harmonic drive model.

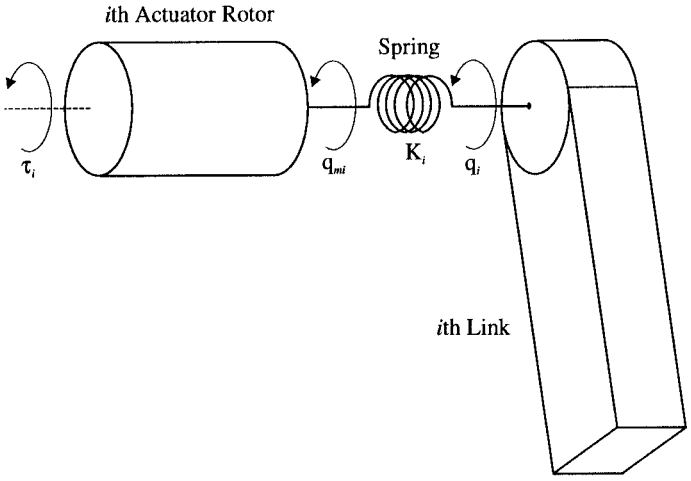

Fig. 1. Schematic representation of the RLFJ robot model.

2 RLFJ ROBOT DYNAMICS

The RLFJ robot model for the ith link is schematically represented by Figure 1. The standard n-DOF, revolute, RLFJ robot is represented by the following dynamic model†

$$M(q)\ddot{q} + V_m(q, \dot{q})\dot{q} + G(q) + F_d\dot{q} = K(q_m - q), \quad (1)$$

$$J\ddot{q}_m + B\dot{q}_m + K(q_m - q) = \tau \quad (2)$$

where $q, q_m \in \Re^n$ denote the link and actuator position vectors, respectively, $M(q) \in \Re^{n\times n}$ is the inertia matrix, $V_m(q, \dot{q}) \in \Re^{n\times n}$ is the centripetal-Coriolis matrix, $G(q) \in \Re^n$ is the gravity vector, and $F_d \in \Re^{n\times n}$ is a positive-definite, diagonal matrix representing the friction coefficients at each joint. The constant, positive-definite, diagonal matrices $K, J, B \in \Re^{n\times n}$ represent the flexibility, inertia, and damping matrices, respectively, of the actuators while the vector $\tau \in \Re^n$ represents the input control torque at each actuator. The dynamic equation given by (1) describes the link dynamics with the transmitted torque between the links and the actuators given by $K(q_m - q)$ (i.e., linear torsional spring) while the dynamic equation given by (2) represents the actuator dynamics.

To formulate the link position tracking control problem, we will use $q_d(t) \in \Re^n$ to represent the desired link position trajectory which is assumed to be bounded (we will also assume that $q_d(t)$ has bounded derivatives up to and including the fourth derivative). The link position tracking error $e(t) \in \Re^n$ and the filtered tracking error[18] $r(t) \in \Re^n$ will be defined as follows

$$e = q_d - q \quad \text{and} \quad r = \dot{e} + \Lambda e \quad (3)$$

where $\Lambda \in \Re^{n\times n}$ is a positive-definite, diagonal, control gain matrix. To facilitate the discussion, we also define the displacement error, denoted by $z(t) \in \Re^n$, as the difference between the actuator and the link position signals as follows

$$z = q_m - q. \quad (4)$$

3 REDUCED-ORDER MODEL-BASED CONTROL

In this section, we use high-gain actuator feedback to develop a reduced-order model for the RLFJ robot dynamics. The reduced-order model greatly simplifies the design of the control in that it reduces the fourth-order RLFJ model to the standard second-order RL model.

† For a list of the assumptions required to formulate the RLFJ robot manipulator dynamics, the reader is referred to reference [5].

https://doi.org/10.1017/S0263574798000113 Published online by Cambridge University Press

Hence, this reduction in the order of the model allows one to utilize previously designed RL controllers as embedded signals during the RLFJ control synthesis.

We begin the control development by using the definitions given in (3) and (4) to rearrange the RLFJ robot dynamics of (1) and (2) into the following convenient form

$$M(q)\dot{r} = -V_m(q, \dot{q})r + W(q, \dot{q}, t) - Kz \tag{5}$$

$$J\ddot{z} + B\dot{z} + Kz = \tau - J\ddot{q} - B\dot{q} \tag{6}$$

where the auxiliary variable $W(q, \dot{q}, t) \in \Re^n$ is defined as follows

$$W(q, \dot{q}, t) = M(q)(\ddot{q}_d + \Lambda\dot{e}) + V_m(q, \dot{q})(\dot{q}_d + \Lambda e) + G(q) + F_d\dot{q}. \tag{7}$$

From the structure of the actuator dynamics given by (6), Spong [5] utilized singular perturbation techniques[19] to motivate the following torque control input

$$\tau = K^{-1}(K + K_{pz})\tau_d - K_{pz}z - K_{dz}\dot{z} \tag{8}$$

where K_{pz}, $K_{dz} \in \Re^{n\times n}$ are positive-definite, diagonal, control gain matrices, and τ_d is an auxiliary signal which will be used to transmit the desired control input to the links. After substituting (8) into (6), we can form the following closed-loop equation

$$J\ddot{z} + (B + K_{dz})\dot{z} + (K + K_{pz})z = K^{-1}(K + K_{pz})\tau_d - J\ddot{q} - B\dot{q}. \tag{9}$$

Without using singular perturbation techniques, we can heuristically develop an understanding of the control structure proposed in (8) by taking the Laplace Transform of (9) and then rearranging the expression to yield

$$Kz(s) = H(s)\mathcal{L}\{\tau_d - K(K + K_{pz})^{-1}(J\ddot{q} + B\dot{q})\} \tag{10}$$

where the effects of the initial conditions have been neglected, $H(s) \in \Re^{n\times n}$ is a diagonal transfer function matrix given by

$$H(s) = (Js^2 + (B + K_{dz})s + (K + K_{pz}))^{-1}(K + K_{pz}), \tag{11}$$

s denotes the Laplace Transform variable, and $\mathcal{L}$ denotes the Laplace Transform operation. The transfer function matrix given by (11) represents n second-order, stable low-pass filters with a dc gain of unity; hence, if the elements of the control gain matrices K_{pz} and K_{dz} are utilized to place the poles of $H(s)$ at a stable location far in the left half plane, then we can use (10) to approximate the transmitted torque (i.e., $Kz(t)$) as follows

$$Kz \cong \tau_d - K(K + K_{pz})^{-1}(J\ddot{q} + B\dot{q}). \tag{12}$$

After substituting the approximate expression of (12) for the transmitted torque into the right-side of (5), we can obtain the following *reduced-order* model for the link position tracking error dynamics

$$\bar{M}(q)\dot{r} = -V_m(q, \dot{q})r + \bar{W}(q, \dot{q}, t) - \tau_d \tag{13}$$

where the auxiliary variables $\bar{M}(q) \in \Re^{n\times n}$ and $\bar{W}(q, \dot{q}, t) \in \Re^n$ are defined as follows

$$\bar{M}(q) = M(q) + (K + K_{pz})^{-1}KJ$$
$$\bar{W}(q, \dot{q}, t) = W(q, \dot{q}, t) + K(K + K_{pz})^{-1}(J(\ddot{q}_d + \Lambda\dot{e}) + B\dot{q}). \tag{14}$$

The motivation for the structure of input control given by (8) is manifested by the form of the link tracking error system given by (13). That is, the open-loop structure given by (13) is reminiscent of the tracking error formulation that Slotine and other researchers[20] used to develop Lyapunov-based controllers during the late nineteen eighties.* Based on this previous work and the second-order nature of (13), a simple design for the embedded signal τ_d which achieves reasonably good tracking is the following proportional derivative (PD) controller

$$\tau_d = K_s r \tag{15}$$

where $K_s \in \Re^{n\times n}$ is positive-definite, diagonal, control gain matrix. If one wishes to increase the link position tracking performance, the structure of (13), standard robot manipulator properties, and a Lyapunov-based stability proof motivate the following nonlinear controller [18] for the embedded signal τ_d

$$\tau_d = \bar{W}(q, \dot{q}, t) + K_s r. \tag{16}$$

To improve computational efficiency, the embedded control signal given by (16) can be modified as follows

$$\tau_d = \bar{W}(q_d, \dot{q}_d, t) + K_s r \tag{17}$$

where the link position and link velocity signals in the feedforward term $\bar{W}(\cdot)$ have been replaced by the desired link position and link velocity signals, respectively. The embedded control signal given by (17) belongs to the so-called Desired Compensation Law family of controllers originally proposed in reference [21].

Remark 1: While it is not the intent of this paper to develop stability proofs for the various control strategies, we should point out that if the control torque signals given by (15), (16), and (17) could be directly applied to the RL dynamic equation given by (1), one obtains semiglobal uniform ultimate bounded, global exponential, and semiglobal† exponential link position/velocity tracking, respectively (see reference [22] for a simplified version of these proofs, experimental results,

* It is easy to show that the matrix $\bar{M}(q)$ is a positive-definite and symmetric matrix and that the matrix $(\frac{1}{2}\dot{\bar{M}}(q) - V_m(q, \dot{q}))$ is skew symmetric.

† Note that *global* exponential tracking for the control algorithm given by (17) can be accomplished by adding an additional nonlinear damping term (see references [21] and [22]).

https://doi.org/10.1017/S0263574798000113 Published online by Cambridge University Press

and the references to other related work). However, the additional set of actuator dynamics and the nonlinearities in the RLFJ model seems to hinder the straightforward establishment of global or semiglobal link position/velocity tracking under the embedded control signals given by (15), (16), and (17) coupled with the actuator control loop of (8).

4 SYNTHESIS OF LINK/ACTUATOR VELOCITY SIGNALS

The class of controllers discussed so far require full-state feedback (FSFB); hence, for the RLFJ robot control problem, we must have access to link position, link velocity, actuator position, and actuator velocity measurements (i.e. q, $\dot{q}$, q_m, and $\dot{q}_m$). While accurate measurement of link position and actuator position is available with optical encoders or resolvers, the use of tachometers for measurement of link velocity and actuator velocity add cost to the robotic system; moreover, tachometer-based measurements of non-constant link/actuator velocity are usually very noisy. For these reasons, the so-called backwards difference algorithm is often utilized to manufacture velocity estimates from position measurements according to following discrete time algorithm

$$\hat{\dot{q}} = \frac{q(pT) - q((p-1)T)}{T} \quad \text{for } p = 1, \ldots, n \qquad (18)$$

where $\hat{\dot{q}} \in \Re^n$ denotes the estimate of link velocity, p represents the sampling instant, T represents the sampling interval, and nT represents the total experiment time (note that the same type of algorithm can be used to generate an estimate of the actuator velocity q_m or an estimate of the time derivative of z). To remove some of the high frequency noise associated with numerically differentiating position, the backwards difference-based velocity estimate is often passed through a low-pass filter before it is utilized in the feedforward/feedback controller.

Many researchers have proposed using a model-based velocity observer as an alternative to the backwards difference algorithm given by (18). The use of a continuous time model-based observer is much more satisfying from a theoretical viewpoint since many researchers[23–27] have illustrated how observer-based velocity estimates can be utilized inside of a model-based control structure without compromising the stability of the closed-loop system. In addition, it seems that previous experimental results[23,24] have suggested that the model-based controller/observer approach exhibits some advantageous robustness properties over the model-based controller/backwards difference approach. Much of this previous work uses the structure of the second-order nonlinear dynamics given by (1) to generate a model-based link velocity observer with the following form

$$\begin{cases} \dot{\hat{q}} = y_q + k_1(q - \hat{q}) \\ \dot{y}_q = M^{-1}(q)(Kz - V_m(q, \hat{\dot{q}})\hat{\dot{q}} - G(q) - F_d\hat{\dot{q}}), \end{cases} \qquad (19)$$

where $\hat{q} \in \Re^n$ denotes the estimate of link position, k_1 is a positive scalar observer control gain, and $y_q \in \Re^n$ is an auxiliary variable which allows the observer to be implemented without using link velocity measurements. After substituting (1) into (6) for $\ddot{q}$, and then replacing $\dot{q}$ with $\hat{\dot{q}}$ a similar procedure can be utilized to develop the following model-based observer which generates an estimate of the time derivative of z

$$\begin{cases} \dot{\hat{z}} = y_z + k_2(z - \hat{z}) \\ \dot{y}_z = J^{-1}[\tau - JM^{-1}(q)(Kz - V_m(q, \hat{\dot{q}})\hat{\dot{q}} \\ \qquad - G(q) - F_d\hat{\dot{q}}) - B\hat{\dot{q}} - B\dot{\hat{z}} - Kz], \end{cases} \qquad (20)$$

where $\hat{z} \in \Re^n$ denotes the estimate of the variable z, k_2 is a positive scalar observer control gain, and $y_z \in \Re^n$ is an auxiliary variable which allows the observer to implemented without using actuator velocity measurements.

Remark 2: If the control torque signal given by (16) (i.e., with all occurrences of $\dot{q}$ replaced by $\hat{\dot{q}}$) could be directly applied to the RL dynamic equation given by (1), it can be shown that one obtains semiglobal exponential link position/velocity tracking (e.g., see reference [23] and [24]). However, the additional set of actuator dynamics, the nonlinearities in the RLFJ model, and the use of velocity estimates generated by (19) and (20) hinder the straightforward establishment of global or semiglobal link position/velocity tracking under the embedded control signals given by (16) coupled with the actuator control loop of (8) (i.e. with all occurrences of $\dot{q}$ and $\dot{z}$ replaced by $\hat{\dot{q}}$ and $\dot{\hat{z}}$, respectively). In the next section of the paper, we discuss how the torque control input can be designed for the full-order RLFJ model to achieve semiglobal link position/velocity tracking despite the use of observed velocity in lieu of actual velocity measurements.

Remark 3: For other related work, the reader is referred to Nicosia et al.[28] who designed several classes of observers which are used to estimate various states of the RLFJ robot dynamic equation, and to Tomei[29] who designed a RLFJ robot observer which asymptotically estimates all the state variables of the robot based on measurements of link position and velocity.

5 FULL-ORDER MODEL-BASED CONTROL

While the FSFB reduced-order controllers given by (8) and (15) or (17) are intuitive and straight-forward to implement, it is a bit unsatisfying from a theoretical viewpoint in that they basically attempt to use a high-gain actuator feedback loop to neutralize the effects of joint flexibility. Over the last four years there has been good deal of activity targeted at the construction of controllers for the full-order RLFJ model. Brogliato et al.[9] provided a survey of various globally stable controllers for RLFJ robots and established a common framework to compare controllers that are based on the integrator backstepping,[30] decoupling-based, and passivity approaches. In [10], Bridges et al. utilized the

https://doi.org/10.1017/S0263574798000113 Published online by Cambridge University Press

backstepping technique to design RLFJ exact model knowledge, adaptive, and robust controllers under a common framework. Lozano et al.[31] developed an adaptive controller without *a priori* knowledge of joint flexibilities that yielded global asymptotic link position tracking. Recently, Tomei[32] designed a robust tracking controller that compensated for unknown friction forces and uncertain kinematic/dynamic parameters while yielding global uniform ultimate bounded (GUUB) link position tracking. Bridges et al.[33] also designed a robust controller which yielded GUUB link position tracking and provided for the use of redundant joint actuators. While the above controllers are relatively computationally intensive, the primary advantage of these full-order controllers over the reduced-order control approach is that *global* link position tracking is achieved despite the effects of joint flexibility. Moreover, it should be noted that all the above RLFJ controllers require FSFB.

For the reasons eluded to earlier, link and actuator velocity measurements are usually not available; therefore, a more interesting control objective is the attainment of link position tracking for the full-order RLFJ dynamics despite the lack of velocity measurements. Similar to the RL output feedback control problem,[23] this RLFJ partial-state feedback (PSFB) control problem is complicated by the dynamic interaction between the velocity observation error system and the closed-loop link position tracking error system (i.e., there does not seem to be a general separation principle for nonlinear systems). Fortunately, the *observed integrator backstepping* technique[30] provides some guidance for these types of control problems. Specifically, in reference [34], Lim et al. presented an exact model knowledge, PSFB, link position tracking controller for RLFJ robots that requires only link position and actuator position measurements. That is, two second-order nonlinear observers (i.e. similar to the observers given by (19) and (20)) were utilized to estimate link velocity and actuator velocity. Based on the structure of the observers and the RLFJ dynamics, a backstepping-type controller, which only requires measurements of link position and actuator position, was developed. A Lyapunov function (composed of link velocity observation error, actuator velocity observation error, link position tracking error, and other auxiliary tracking error signals) along with the nonlinear damping argument [30] were then used to achieve a *semiglobal* exponential stability result for the link position tracking error, link velocity observation error, and actuator velocity observation error during closed-loop operation. Due to its complexity, the form of the control law will be omitted; however, the reader is referred to reference [34] for the control structure and stability analysis.

Remark 4: Over the past two years, a few other full-order model-based RLFJ controllers have been proposed which do not require FSFB. For example, Qu[35] provided a PSFB RLFJ robot controller which requires only measurement of link position and link velocity. Recently, Nicosia and Tomei proposed an exact model knowledge controller[36] which only require link position measurements while delivering semi-global asymptotic link position tracking (i.e., an output feedback RLFJ robot controller). Lim et al.[37] proposed an adaptive controller which achieved semi-global asymptotic link position tracking, compensated for parametric uncertainty throughout the entire system, and only required measurements of link position and actuator position.

6 EXPERIMENTAL SETUP AND RESULTS

An IMI, 2-DOF direct-drive (DD) planar robot[38] was modified to approximate the model of a RLFJ robot described by (1) and (2). The modifications include a hub to decouple the motion of each link actuator from the corresponding link and a pair of extension springs to recouple the motion of the actuators with the link through a flexible connection. The hub, mounted between the rotor of the link actuator and the link, consists of an inner spindle that supports an outer housing through two opposing tapered roller bearings as shown in Figure 2. The inner spindle is attached to the link actuator and the outer housing is connected to the link. Installations of the hubs allows the links to rotate free of the link actuators. The extension springs provide

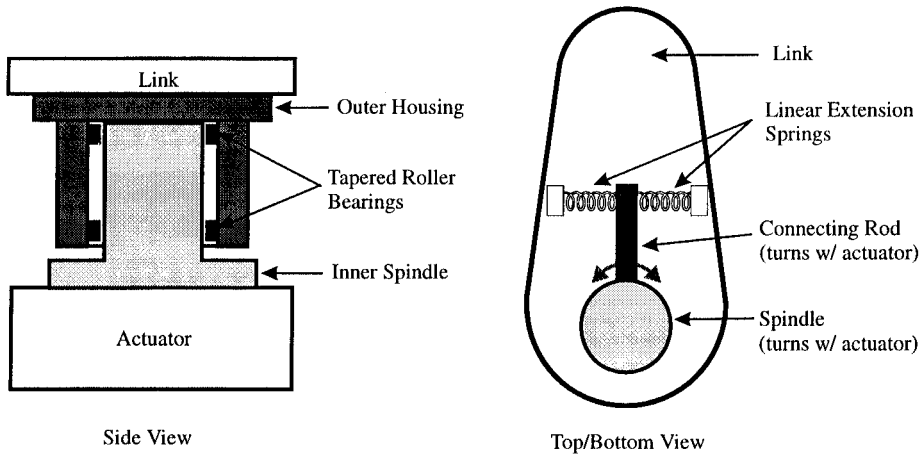

Fig. 2. Schematic representation of the design modifications to the IMI robot.

https://doi.org/10.1017/S0263574798000113 Published online by Cambridge University Press

Table I
Control gains

PD-OB	*DC-BD*	*DC-OB*	*PS-OB*
K_s = diag {60.0, 3.0}	K_s = diag {19.0, 0.99}	K_s = diag {5.1, 1.28}	K_s = diag {6.1, 0.54}
Λ = diag {0.233, 0.142}	Λ = diag {16.0, 39.0}	Λ = diag {116.0, 33.0}	k_1 = diag {29.0, 20.0}
K_{Pz} = diag {15.0, 1.0}	K_{Pz} = diag {57.0, 13.0}	K_{Pz} = diag {120.0, 10.5}	k_2 = diag {41.0, 28.0}
K_{Dz} = diag {6.0, 0.3}	K_{Dz} = diag {2.6, 0.15}	K_{Dz} = diag {1.8, 0.22}	k_3 = diag {6.8, 5.2}
		k_1 = diag {40.0, 115.0}	k_4 = diag {5.9, 1.0}
		k_2 = diag {60.0, 260.0}	k_5 = diag {5.9, 0.4}
			k_n = 0.0008

the approximation to joint flexibility as shown in Figure 2. As the link actuator turns the spindle and connecting rod, a torque is applied to the link through the extension springs that is roughly proportional to the difference between the actuator and link positions. A RLFJ robot constructed in this manner exhibits a minor deviation from the model in (1) and (2). Specifically, the torsional spring constant is only approximately linear over a limited range of displacement between the actuator and the link; however, plots of the displacement versus the applied torque (see Figure 3) illustrate a linear spring constant relationship over the range of motion used in the experiments. That is, the approximate slopes of the curves in Figure 3 yield linear torsional spring constants of 363 Nm/rad for the base joint and 22 Nm/rad for the elbow joint.

The objective of the experimental work was to evaluate the link tracking performance of three reduced-order control algorithms and the full-order controller presented in reference [34]. Specifically, the four evaluated controllers were: (i) PD controller with backwards difference/filtering (denoted as *PD-BD*) given by (8), (15), and (18), (ii) Desired Compensation controller with backwards difference/filtering (denoted as *DC-BD*) given by (8), (17), and (18), (iii) Desired Compensation controller with model-based observers (denoted by *DC-OB*) given by (8), (17), (19), and (20), and (iv) PSFB controller with model-based observers (denoted by *PS-OB*) given in reference [34]. The controllers were implemented on the modified IMI, 2-DOF DD RLFJ planar robot described above. A brief description of the hardware/software components of the experimental setup shown in Figure 4 is given below. (i) a Intel 486 host PC containing a windows-based user interface software with on-line plotting capability, (ii) a TMS320C30 real-time DSP board mounted in the host PC which is responsible for data acquisition and execution of the control algorithm, (iii) two NSK torque-controlled amplifiers, and (iv) NSK Megatorque motors RS1410 and RS0608 to actuate the base and elbow links, respectively, and (v) two IMI DS-2 encoder interface boards utilized in conjunction with two NSK

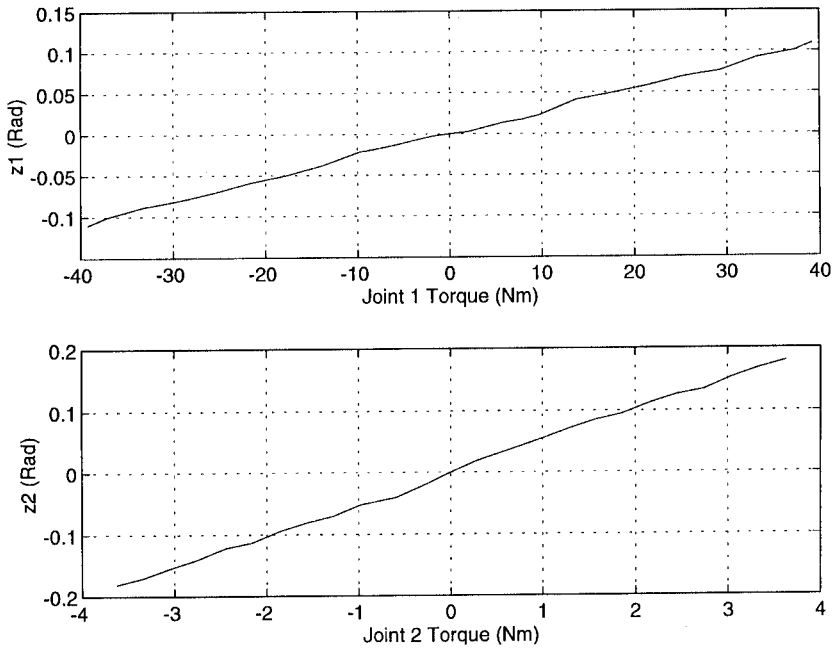

Fig. 3. Flexibility coefficients for the base and elbow joints.

https://doi.org/10.1017/S0263574798000113 Published online by Cambridge University Press

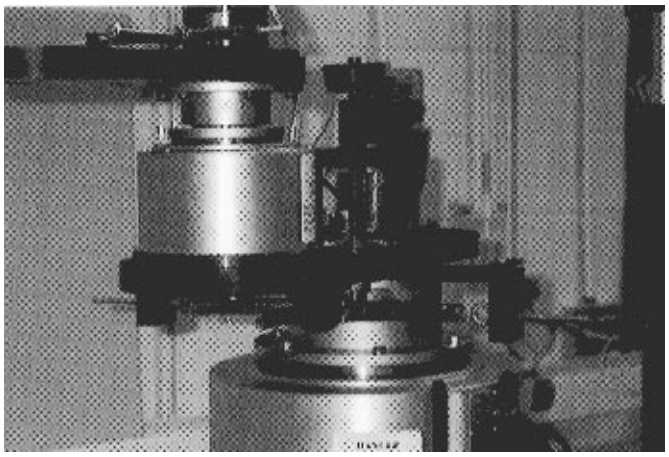

Fig. 4. Picture of the 2-DOF RLFJ robot testbed.

resolver/encoders and two Gurley encoders to measure actuator and link position, respectively.

Based on the form of (1) and (2) and several standard test procedures, the dynamic model for the modified IMI, 2-DOF DD RLFJ planar robot was determined to be

$$M(q) = \begin{bmatrix} 5.68 + 0.20c_2 & 0.43 + 0.01c_2 \\ 0.43 + 0.10c_2 & 0.43 \end{bmatrix} \text{kg-m}^2/\text{rad},$$

$$V_m(q, \dot{q}) = \begin{bmatrix} -0.10s_2\dot{q}_2 & -0.10s_2(\dot{q}_1 + \dot{q}_2) \\ 0.10s_2\dot{q}_1 & 0 \end{bmatrix} \text{Nm-sec/rad},$$

$$G(q) = 0 \text{ N},$$

$$F_d = \text{diag}\{0.69, 0.10\} \text{ Nm-sec/rad},$$

$$K = \text{diag}\{363.0, 22.0\} \text{ Nm/rad},$$

$$J = \text{diag}\{2.49, \quad 0.20\} \text{ kg-m}^2/\text{rad},$$

$$B = \text{diag}\{1.27, 0.78\} \text{ Nm-sec/rad}$$

where c_2 denotes cos (q_2), and s_2 denotes sin (q_2).

For all of the experiments, we utilized the following *smooth*-start sinusoid for the desired link position trajectories

$$q_{d1}(t) = q_{d2}(t) = \sin(2.4t(1 - e^{-0.1t^4})) \text{ rad}.$$

The sampling period at which each controller was run was: *PD-BD*, 400 μsec; *DC-BD*, 500 μsec; *DC-OB*, 350 μsec; and *PS-OB*, 800 μsec. All of the control gains were tuned until the best link position tracking performance was achieved. It is important to note that while many of the controller/observer gains were defined as scalars (e.g. the observer gains k_1 and k_2 defined in (19) and (20) are often defined as scalars for simplicity or for technical reasons), we observed better link position tracking performance by using separate control gain values for each link. Table I summarizes the control gains used for the four controllers. Figure 5–8 illustrate the link position tracking errors for the *PD-BD*, *DC-BD*, *DC-OB*, and *PS-OB* controllers, respectively.* Since the magnitude of the input torques were similar for all controllers, we have included in Figure 9 plots of the

* Note that the same vertical scale has been used to facilitate the comparison of the tracking errors.

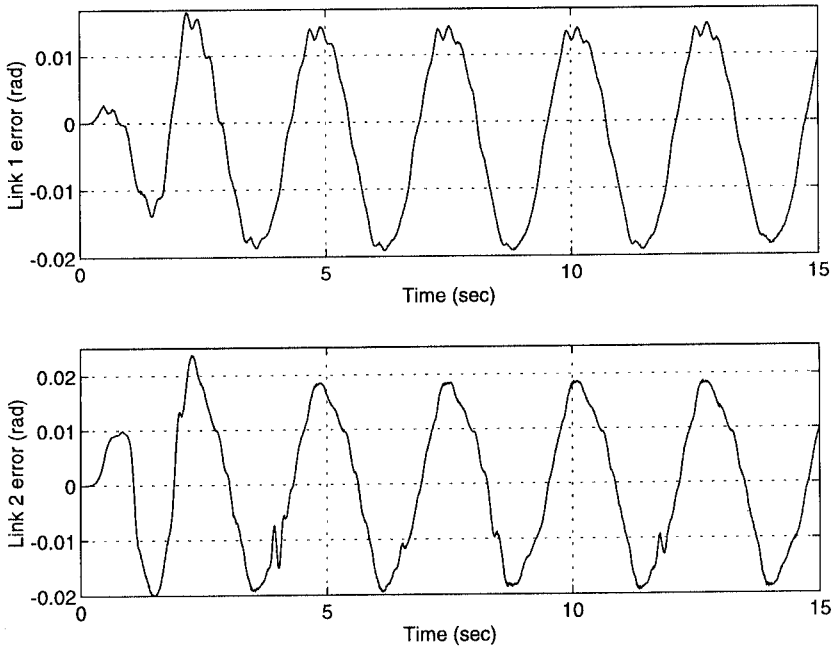

Fig. 5. Link position tracking errors – PD-BD controller.

https://doi.org/10.1017/S0263574798000113 Published online by Cambridge University Press

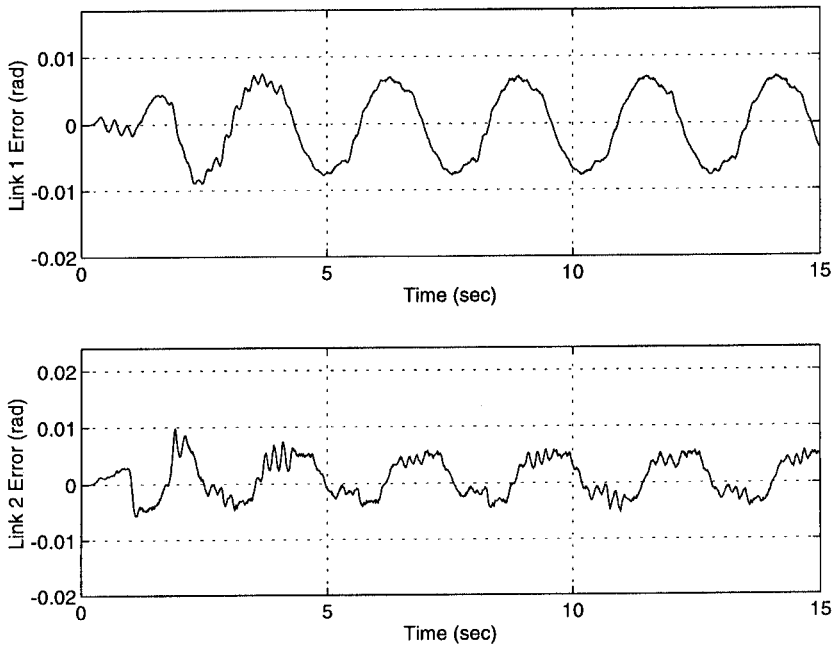

Fig. 6. link position tracking errors – DC-BD controller.

input torques for the *PS-OB* controller only. In Figure 10, we have plotted the actuator/link displacements (i.e. z) for the *PS-OB* controller to illustrate that they are within the displacement range of the linear spring assumption (see Figure 3) (the displacements for all other controllers were similar). Table II summarizes the link position tracking performance of the four controllers by showing the maximum absolute value of the steady-state position tracking errors and the integral of the square of the tracking errors.

The experimental results indicate that relatively good link position tracking can be obtained with a linear PD link signal embedded inside of a linear PD actuator controller (i.e. *PD-BD* controller). By augmenting the control law with a desired compensation feedforward term (i.e. *DC-BD* and *DC-OB* controllers), a significant improvement in the link position tracking performance was achieved. A slight improvement was obtained by utilizing the velocity observer in place of the backwards difference-based velocity scheme in the *DC* controller (we believe that different selections of the desired link position trajectory would make this improvement better manifest itself). Some modest improvements in the maximum absolute value of the steady-state position

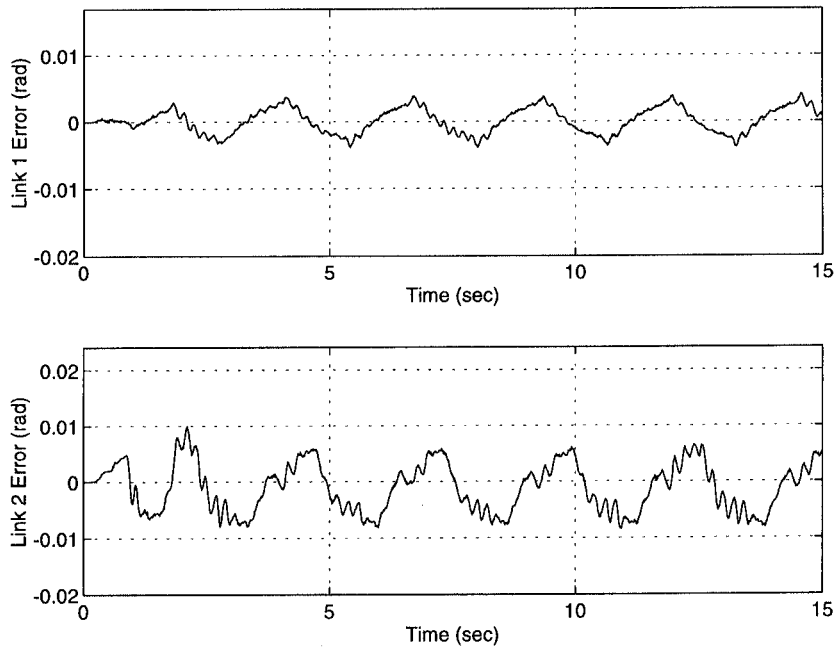

Fig. 7. Link position tracking errors – DC-OB controller.

https://doi.org/10.1017/S0263574798000113 Published online by Cambridge University Press

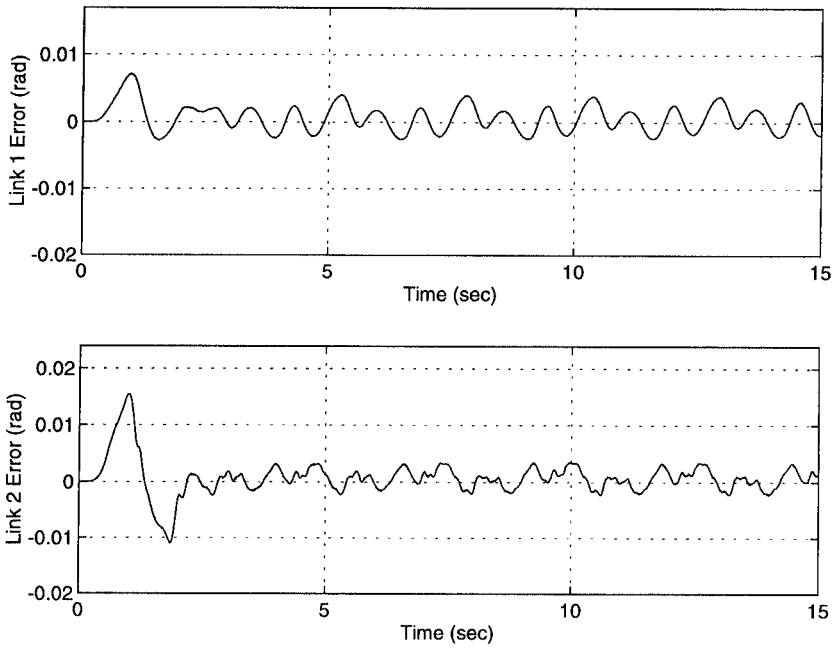

Fig. 8. Link position tracking – PS-OB controller.

tracking errors was obtained by the *PS-OB* controller, however, this improvement was achieved at the expense of a significantly more complex control algorithm.

7 CONCLUSIONS

In this paper, we have presented an experimental evaluation of three reduced-order and one full-order model-based, link position tracking controllers for RLFJ robots. An experimental testbed composed of a 2-DOF direct-drive RLFJ robot was built to approximate the linear spring, flexible joint model introduced in [5], and hence, ensure that backlash and harmonic drive effects do not contaminate the experimental results. While the objective of the paper was not to present an exhaustive experimental comparison of the controllers, we believe the results do provide a good indication of the controllers' relative performance when applied to an actual RLFJ robot system. Based on the experimental results, the full-order model-based control algorithm produced the best tracking performance as one would theoretically expect. However, the improvement in performance over the reduced-order scheme composed of a Desired Compensation-type controller embedded inside a PD actuator controlller might not be significant enough to justify the implementation of such a computationally expensive control algorithm.

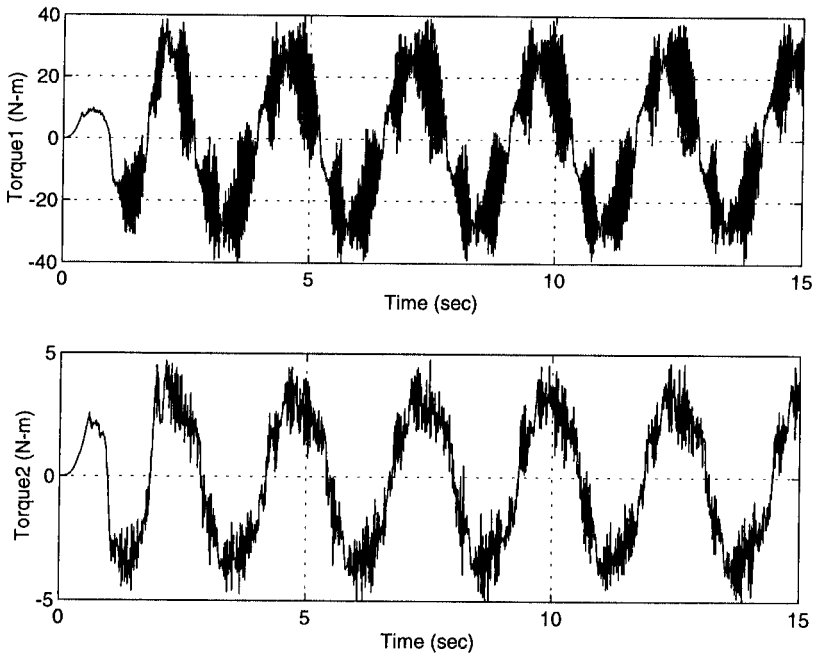

Fig. 9. Input control torques – PS-OB controller.

https://doi.org/10.1017/S0263574798000113 Published online by Cambridge University Press

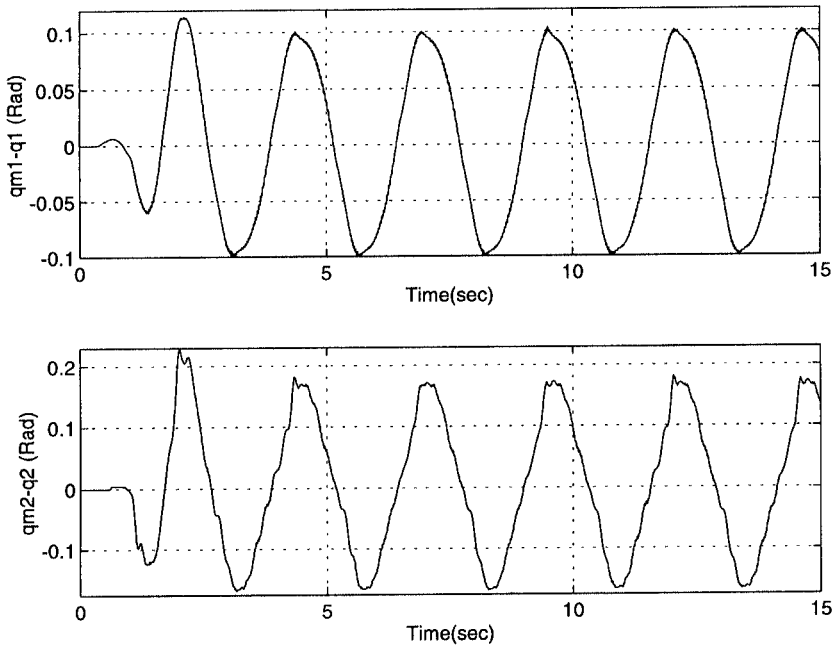

Fig. 10. Actuator/link displacements – PS-OB controller.

Table II
Link position tracking performance

	PD-BD	*DC-BD*	*DC-OB*	*PS-OB*
$\|e_{1ss}\|_{max}$ (rad)	0.0192	0.0078	0.0040	0.0038
$\|e_{2ss}\|_{max}$ (rad)	0.0218	0.0052	0.0078	0.0035
$\int_0^{15} e_1^2(t)dt$	2.011×10^{-3}	3.700×10^{-4}	5.240×10^{-5}	6.635×10^{-5}
$\int_0^{15} e_2^2(t)dt$	2.358×10^{-3}	1.755×10^{-4}	3.017×10^{-4}	1.561×10^{-4}

References

1. M.S. de Queiroz, S. Donepudi, T. Burg and D.M. Dawson, "Experimental Evaluation of Link Position Tracking Controllers for Rigid-Link Flexible-Joint Robots" *Proc. IEEE Conf. Decision and Control,* Kobe, Japan (Dec., 1996) pp. 4092–4097.
2. A. Liegeois, E. Dombre and P. Borrel, "Learning and Control for a Compliant Computer-Controlled Manipulator" *IEEE Trans. Automatic Control* **AC-25,** No. 6, pp. 1097–1102 (Dec., 1980).
3. W. Sunada and S. Dubowsky, "On the Dynamic Analysis and Behavior of Industrial Robotic Manipulators with Elastic Members" *ASME J. Mech. Transm. Autom. Design* **105,** No. 1, 42–51 (Mar., 1983).
4. L. Sweet and M. Good, "Redefinition of the Robot Motion Control Problem: Effects of Plant Dynamics, Drive System Constraints, and User Requirements" *Proc. IEEE Conf. Decision and Control,* Las Vegas, NV (1984) pp. 724–730.
5. M. Spong, "Modeling and Control of Elastic Joint Robots" *ASME J. Dynamic Systems, Measurement, and Control* **109,** 310–319 (Dec., 1987).
6. F. Ghorbel, J.Y. Hung and M.W. Spong, "Adaptive Control of Flexible Joint Manipulators" *IEEE Control Systems Mag.* **9,** No. 7, 9–13 (Dec., 1991).
7. M. Spong, "Adaptive Control of Flexible Joint Manipulators: Comments on Two Papers" *Automatica* **31,** No. 4, 585–590 (Apr., 1995).
8. J.Y. Hung, "Control of Industrial Robots that Have Transmission Elasticity" *IEEE Trans. Industrial Electronics* **38,** No. 6, 421–427 (Dec., 1991).
9. B. Brogliato, R. Ortega and R. Lozano, "Globally Stable Nonlinear Controllers for Flexible Joint Manipulators: A Comparative Study" *Automatica* **31,** No. 7, 941–956 (July, 1995).
10. M.M. Bridges, D.M. Dawson and C.T. Abdallah, "Control of Rigid-Link Flexible-Joint Robots: A Survey of Backstepping Approaches", *J. Robotic Systems* **12,** No. 3, 199–216 (Mar., 1995).
11. B. Brogliato, A. Pastore, D. Rey and J. Barnier, "Experimental Comparison of Nonlinear Controllers for Flexible Joint Manipulators" *Proc. IEEE Int. Conf. Robotics and Automation,* Minneapolis, MN (Apr., 1996) pp. 1121–1126.
12. M. Margulis and D. Volkov, "Calculation of the Torsional Rigidity of a Harmonic Power Drive with a Disc Generator" *Soviet Engineering Research* **7,** No. 6, 17–20 (1987).
13. D. Volkov and Y. Zubkov, "Vibrations in a Drive with Harmonic Gear Transmissions" *Russian Engineering Journal* **58,** No. 5, 11–15 (1978).
14. T.D. Tuttle, "Understanding and Modeling the Behavior of a Harmonic Drive Gear Transmission" *Masters Thesis* (MIT, Dept. of Mechanical Engineering, May, 1992).
15. B. Yu, "Effect of Teeth on the Rim Rigidity of the Flexible Gear Wheel of a Harmonic Drive", *Russian Engineering Journal* **58,** No. 7, 29–32 (1978).
16. M.M. Bridges, D.M. Dawson and S.C. Martindale, "An Experimental Study of Flexible Joint Robots with Harmonic Drive Gearing" *Proc. IEEE Conf. Control Applications,* Vancouver, Canada (Sept., 1993) pp. 499–504.
17. M.M. Bridges and D.M. Dawson, "Redesign of Robust Controllers for Rigid-Link Flexible-Joint Robotic Manipulators Actuated with Harmonic Drive Gearing" *IEE Proc.*

https://doi.org/10.1017/S0263574798000113 Published online by Cambridge University Press

Control Theory and Applications **142,** No. 5, 508–514 (Sept., 1995).
18. J. Slotine and W. Li, *Applied Nonlinear Control* (Prentice Hall Co., Englewood Cliff, NJ, 1991).
19. P. Kokotovic, H. Khalil and J. O'Reilly, *Singular Perturbation Methods in Control: Analysis and Design* (Academic Press, London, 1986).
20. M.W. Spong, "Control of Flexible Joint Robots: A Survey" *Coordinated Science Laboratory Report UILU-ENG-90-2203 DC-116* (Univ. of Illinois at Urbana-Champaign, Feb., 1990).
21. N. Sadegh and R. Horowitz, "Stability and Robustness Analysis of a Class of Adaptive Controllers for Robotic Manipulators" *Int. J. Robotics Research* **9,** No. 9, 74–92 (June, 1990).
22. M.S. de Queiroz, D. Dawson and T. Burg, "Reexamination of the DCAL Controller for Rigid Link Robots" *Robotica* **14,** Part 1, 41–49 (Jan./Feb., 1996).
23. H. Berghuis and H. Nijmeijer, "A Passivity Approach to Controller–Observer Design for Robots" *IEEE Trans. Robotics and Automation* **9,** No. 6, 740–754 (Dec., 1993).
24. S.Y. Lim, D.M. Dawson and K. Anderson, "Re-examining the Nicosia–Tomei Robot Observer-Controller from a Backstepping Perspective" *IEEE Trans. Control Systems Technology* **4,** No. 3, 304–310 (May, 1996).
25. S. Nicosia and P. Tomei, "Robot Control by Using Only Joint Position Measurements" *IEEE Trans. Automatic Control* **35,** No. 9, 1058–1061 (Sept., 1990).
26. Z. Qu, D. Dawson, J. Dorsey and J. Duffie, "Robust Estimation and Control of Robotic Manipulators" *Robotica* **13,** Part 3, 223–231 (1995).
27. J. Yuan and Y. Stepanenko, "Robust Control of Robotic Manipulators without Joint Velocity Feedback" *Int. J. Robust and Nonlinear Control* **1,** 203–213 (1991).
28. S. Nicosia, P. Tomei and A. Tornambe, "A Nonlinear Observer for Elastic Robots" *IEEE J. Robotics and Automation* **4,** No. 1, 45–52 (Feb., 1988).
29. P. Tomei, "An Observer for Flexible Joint Robots" *IEEE Trans. Automatic Control* **35,** No. 6, 739–743 (June, 1990).
30. P. Kokotovic, "The Joy of Feedback: Nonlinear and Adaptive" *IEEE Control Systems Mag.* **12,** 7–17 (June, 1992).
31. R. Lozano and B. Brogliato, "Adaptive Control of Robot Manipulators with Flexible Joints" *IEEE Trans. Automatic Control* **37,** No. 2, 174–181 (Feb., 1992).
32. P. Tomei, "Tracking Control of Flexible Joint Robots with Uncertain Parameters and Disturbances" *IEEE Trans. Automatic Control* **39,** No. 5, 1067–1072 (May, 1994).
33. M.M. Bridges, D.M. Dawson, Z. Qu and S.C. Martindale, "Robust Control of Rigid-Link Flexible-Joint Robots with Redundant Actuators" *IEEE Trans. Systems, Man, and Cybernetics* **24,** No. 7, 961–970 (July, 1994).
34. S.Y. Lim, J. Hu, D.M. Dawson and M. Queiroz, "A Partial State Feedback Controller for Trajectory Tracking of Rigid-Link Flexible-Joint Robots using an Observed Backstepping Approach" *J. Robotic Systems* **12,** No. 11, 727–746 (Nov., 1995).
35. Z. Qu, "Input–Output Robust Tracking Control Design for Flexible Joint Robots" *IEEE Trans. Automatic Control* **40,** No. 1, 78–83 (Jan., 1995).
36. S. Nicosia and P. Tomei, "A Tracking Controller for Flexible Joint Robots Using Only Link Position Feedback" *IEEE Trans. Automatic Control* **40,** No. 5, 885–890 (May, 1995).
37. S. Lim, D. Dawson, J. Hu and M. Queiroz, "An Adaptive Link Position Tracking Controller for Rigid-Link Flexible-Joint Robots without Velocity Measurements" *IEEE Trans. Systems, Man, and Cybernetics* **27-B,** No. 3, 412–427 (May, 1997).
38. *Direct Drive Manipulator Research and Development Package Operations Manual* (Integrated Motion Inc., Berkeley, CA, 1992).

https://doi.org/10.1017/S0263574798000113 Published online by Cambridge University Press